Available online at www.sciencedirect.com
ScienceDirect
Sensors and Actuators B 117 (2006) 431–436
SENSORS AND ACTUATORS B CHEMICAL
www.elsevier.com/locate/snb

Optical detection for droplet size control in microfluidic droplet-based analysis systems

Nam-Trung Nguyen *, Sumantri Lassemono, Franck Alexis Chollet

School of Mechanical and Aerospace Engineering, Nanyang Technological University, 50 Nanyang Avenue, Singapore 639798, Singapore

Received 11 May 2005; accepted 2 December 2005
Available online 18 January 2006

Abstract

This paper reports on a hybrid polymeric microfluidic device with optical detection for droplet-based systems. The optical part of the device is integrated by a hybrid concept. The microfluidic structures were fabricated using CO_2 laser on poly methylmethacrylate (PMMA) substrate. The microfluidic network consists of two microchannels for forming droplets of an aqueous liquid in an immiscible carrier liquid. The optical component consists of two optical fibers for guiding laser light from the source, through the detection point, to a photo diode. The formed droplets pass the detection point and diffract the incoming laser light. The detected signal at the photo diode can be used for evaluating droplet size, droplet shape, and droplet formation frequency. The device can detect very high formation frequencies, which are not detectable using a conventional CCD camera/microscope setup.

Keywords: Droplet microfluidics; Polymeric micromachining; Lab on chip; Optical detection

1. Introduction

Droplet-based microfluidics has been emerging in the recent years because of its potential and apparent advantages. One of the key advantages of this concept is the small sample volume on the order of picoliters and nanoliters. A number of concepts such as thermocapillary [1], electrowetting [2,3], or multi-phase flow [4] can be used for generating and controlling of droplets. Droplet formation based on multi-phase flow is easy to implement in a continuous-flow system. In this case, the fluidic system consists of two immiscible phases such as an aqueous liquid and an oil. The balance between the shear stress of the carrier flow and the interfacial tension between the two liquid phases leads to the formation of droplets [5].

Systems generating micro-droplets have been successfully used as microreactors for chemical analysis and protein crystallization [4]. Furthermore, dispersed droplets of one liquid in a second liquid can form an emulsion, which have many applications in food industries and cosmetic industries. Emulsion is important for packaging small amounts of fluid and other active ingredients such as drugs. Encapsulation of nanoliter droplets can also be achieved with a double emulsion. An intermediate fluid layer works as an additional barrier between the inner fluid and the carrier fluid. Recent interest of the research community on double emulsion in micro-scale shows its potential significance [6,7]. Since the droplet's size and its other properties are important for the actual application, a detection system for the micro-droplets is vital for providing a feedback signal to the droplet formation process.

Most of the recent works on micro-droplets only report devices made of polydimethylsiloxane (PDMS) and glass using external syringe pumps. A microscope and a CCD-camera are usually used for characterization of the droplets. The whole setup is rather bulky and the collected data are difficult to analyze automatically. Furthermore, expensive high-speed camera and synchronized strobe illumination are needed for capturing processes with droplet frequencies on the order of tens Hertz and above.

In this paper, we present a poly methylmethacrylate (PMMA) device for droplet formation. The device has a hybrid-integrated optical system for evaluating parameters of the droplet formation process such as the formation frequency, droplet size, and contact angles of the receding and advancing edges. Very high formation frequency can be detected by this device. The paper

* Corresponding author. Tel.: +65 67904457; fax: +65 67911859.
E-mail address: mntnguyen@ntu.edu.sg (N.-T. Nguyen).

0925-4005/$ – see front matter © 2005 Elsevier B.V. All rights reserved.
doi:10.1016/j.snb.2005.12.010

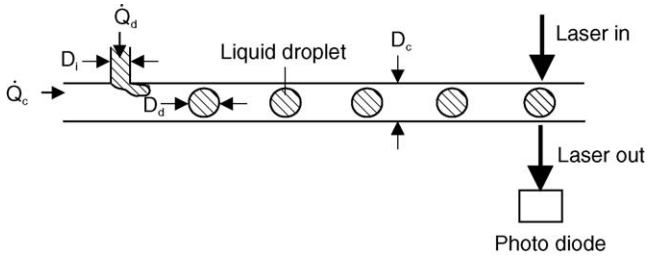

Fig. 1. Concept of formation and detection of liquid droplets in a microchannel.

first discusses a simple theory on droplet formation to identify the key parameters of this process. Next, the fabrication of the device and experimental results are presented and compared with the theory.

2. Formation and optical detection of micro-droplets

Fig. 1 depicts a simple model of the formation process of a liquid droplet in another immiscible carrier fluid. The following model only serves the purpose of understanding the relations between key parameters such as droplet size, formation frequency, flow rates, and most importantly the interfacial tension between the two liquid phases. The model assumes a fixed flow rate ratio between the aqueous liquid and carrier liquid ($\alpha = \dot{Q}_d/\dot{Q}_c$). We further assume that the droplet size is small ($\alpha \ll 1$). Since the droplets are formed in micro-scale and the flows are in steady state, mass related forces such as inertial force, momentum force and buoyancy force are neglected in this model. If the aqueous liquid contents a surfactant, the surfactant concentration at the droplet surface is not uniformly distributed during the process of droplet growth. The distributed surfactant concentration leads to a gradient of interfacial tension on the droplet surface. This interfacial tension gradient in turn induces a Marangoni force on the droplet. If the surfactant solution is diluted, the Marangoni force is assumed to be small and negligible. The injection channel and the carrier channel are both assumed to be cylindrical.

Considering all the above assumptions, the force balance includes only the drag force of the carrier flow and the interfacial tension at the injection port:

$$\begin{aligned} F_{\text{drag}} &= F_{\text{interfacial tension}} \\ \tfrac{1}{2} C_D \rho U_c^2 A_D &= C_S \pi D_i \sigma \end{aligned} \tag{1}$$

where ρ_c, U_c, A_D, D_i, and σ are the density of the carrier fluid, the average velocity of the carrier flow, the effective drag surface, the diameter of the injection port, and the interfacial tension, respectively. In addition, C_D and C_S are the drag coefficient and the coefficient for the interfacial tension. The coefficient C_S depends on the contact angle and the shape of the injection port. In this model C_S is assumed to be constant. We assume for C_D the drag coefficient of a hard sphere at a low Reynolds number Re:

$$C_D = \frac{24}{Re}. \tag{2}$$

The effective drag interfacial A_D grows with the droplet. Assuming that the droplet is a sphere, the effective drag surface at the detachment moment is:

$$A_D = \frac{\pi D_d^2}{2} \tag{3}$$

where D_d is the diameter of the generated droplet. Initially, the interfacial tension is large enough to keep the small droplet at the injection port. At the detachment moment, the continuous droplet growth makes the drag force large enough to release the droplet. Substituting (3) into (1) results in the droplet diameter:

$$D_d = 2\sqrt{\frac{C_S}{C_D} D_i \frac{\sigma}{\rho_c U_c^2}} \tag{4}$$

The formation frequency can be estimated from the flow rate of the aqueous liquid $\dot{Q}_d$ and the droplet volume V_d as:

$$f = \frac{\dot{Q}_d}{V_d} \tag{5}$$

Using the droplet diameter D_d and the relation $\dot{Q}_d = \alpha \dot{Q}_c$, the formation frequency in (5) can be expressed as:

$$f = \frac{3\alpha D_c^2}{16((C_S/C_D)D_i)^{\frac{3}{2}}} \frac{\rho_c^{\frac{3}{2}} U_c^4}{\sigma^{\frac{3}{4}}} \tag{6}$$

where D_c is the diameter of the carrier channel. Eq. (6) shows a nonlinear relation between the formation frequency and the average carrier's velocity ($f \propto U_c^4$) or flow rate ($f \propto \dot{Q}_c^4$). Furthermore, if the Marangoni force is considered in Eq. (1), and if the surfactant concentration is high, there will be an additional term for such force in the numerator of (6), resulting in a higher formation frequency.

Our droplet-based microfluidic device consists of two parts: a microchannel system for droplet formation and an optical detection system, Fig. 1. The microfluidic network consists of a large carrier channel and a small injection channel. The aqueous liquid enters through the injection channel, while an immiscible carrier liquid is introduced into the carrier channel. The two channels form a T-junction, at which droplet formation occurs. After droplets are formed and stabilized, they can be detected at a downstream position. The detection system is based on the optical concept. Laser light is guided into the microchannel by an optical fiber. After passing through the microchannel, the light is received at the other side by a second optical fiber which leads the laser to an optical sensor. The passing-by droplets change the intensity of the light due to diffraction and absorption. Thus the size and shape of the droplet can be well recorded as the time signal of the optical sensor.

On the receiving side of the microchannel, the laser light diffracted by the propagation and by the different interfaces must enter the fiber within a fixed angle. This angle depends on the optical fiber's numerical aperture (NA) and the refractive indices of the fiber's core and cladding. In our later experiments, the optical fiber had a numerical aperture of 0.22. Theoretically, the maximum angle of the incident light in our device is 12.7°.

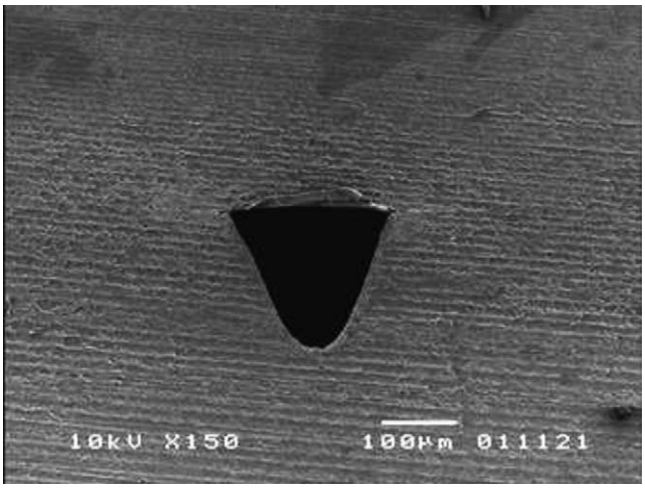

Fig. 2. Cross section of the laser machined microchannel.

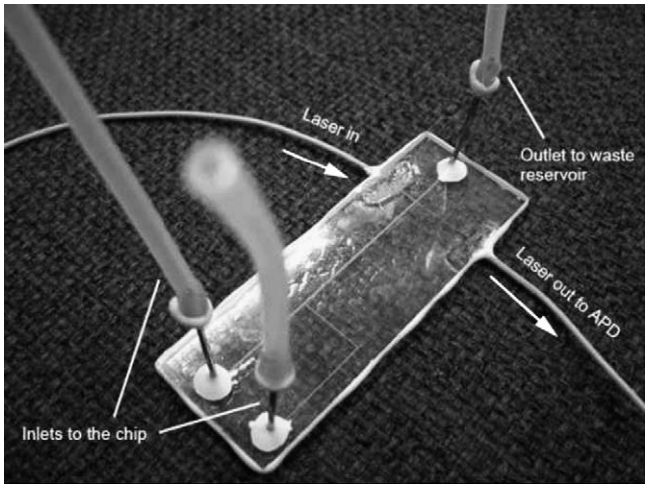

Fig. 4. Microfluidic device for droplet formation and optical detection.

Beyond this angle, light would be refracted away from the fiber and would not reach the photo detector.

3. Device fabrication and experimental setup

Our polymeric technology is based on direct writing on PMMA using a CO_2 laser beam. Because the substrate material is ablated by thermal energy, the microchannel cross section has the same shape as the beam intensity distribution, which has a typical Gaussian shape, Fig. 2. The width and depth of the ablated channel depend on the laser power and the beam speed. In our device, the injection channel and the guides for inserting the optical fibers are 175 μm in width and 205 μm in depth. The carrier channel is larger with a width of 340 μm and a depth of 340 μm. Fig. 3 shows the T-junction of the injection channel and the carrier channel.

Our device has three fluidic interconnects, two for the inlets and one for the outlet. Close to the outlet, two guides are machined into the substrate for aligning the two glass fibers. These fibers are used for optical detection of the micro-droplets. The optical fiber (AFS105/125Y from THORLABS Inc.) has a core diameter of 105 μm, a clad diameter of 125 μm, a buffer diameter of 250 μm, a numerical aperture of 0.22. After positioning the fibers, the whole device is bonded thermally at a temperature above the glass temperature of PMMA. Fig. 4 depicts the complete device.

For detecting the droplets, one glass fiber is positioned and aligned to a laser source (laser diode, $\lambda = 635$ nm), the other fiber is connected to an avalanche photodiode module (APD, C5460-01, Hamamtsu, Japan). The complete experimental setup is shown in Fig. 5.

In our experiments, oil with a viscosity of 6.52×10^{-2} Pa s enters the channel through the inlet for carrier liquid. The other inlet is for the aqueous liquid. The aqueous liquids are pure DI-water (viscosity of approximately 10^{-3} Pa s) or diluted detergent solutions. A liquid detergent was diluted in DI water with different volume ratios to form our test samples. Both carrier liquid and aqueous liquid are driven by a syringe pump. The diameters of the syringes have a fixed ratio of 1:2. Thus, the total flow rate of oil is two times the flow rate of water. To relate the output signal to the droplet parameters, the images of droplet forma-

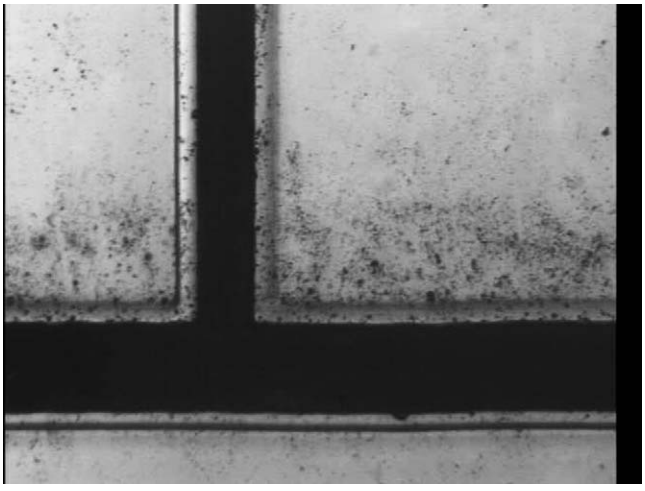

Fig. 3. Microchannels at the T-junction.

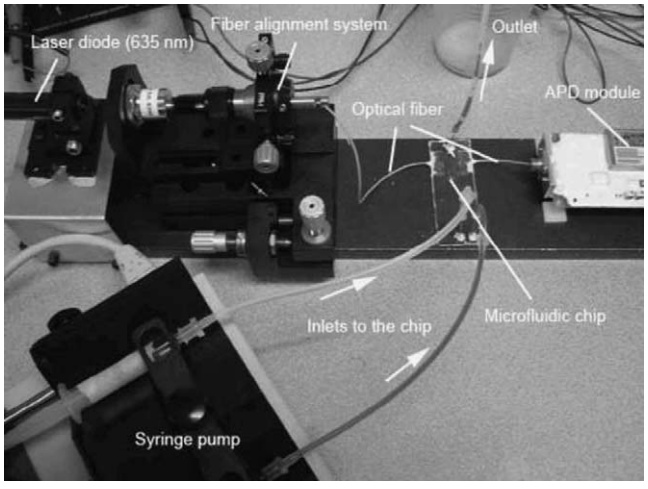

Fig. 5. Experimental setup for droplet formation and detection in a microfluidic device.

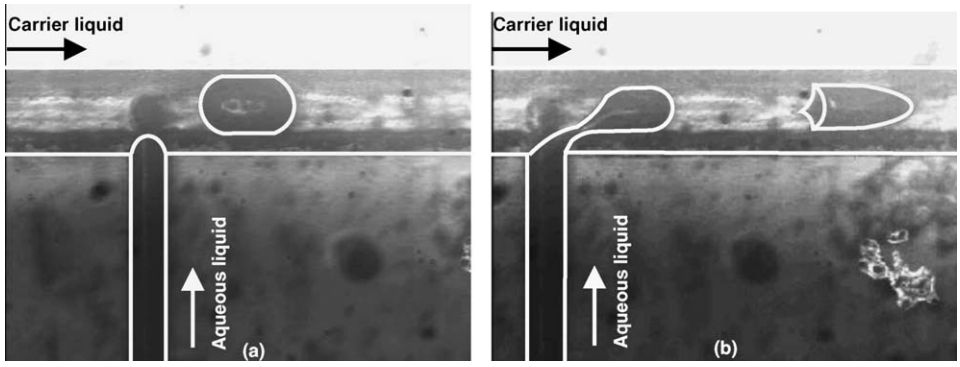

Fig. 6. Droplet formation in the microchannel (flow rate of the aqueous liquid is 30 μL/h): (a) pure DI water, (b) detergent diluted in DI water, volume ratio of 12.5×10^{-3}.

tion are captured with a CCD camera and a microscope system. The CCD sensor has a fixed exposure time of 20 ms. Thus, only formation frequencies on the order of 1 Hz can be observed and recorded clearly. The output signal of the optical detection system is recorded with a digital oscilloscope and transferred to a PC for further evaluations.

4. Results and discussion

4.1. Droplet shapes

Fig. 6 shows the typical micro-droplet formed inside the microchannel. The advancing and receding edge of the droplet have different radii of curvature. Using the CCD camera, the advancing and receding edge of a water droplet can not be clearly differentiated. The difference between the two edges is more apparent when the interfacial tension decreases with detergent. Firstly, the receding side of the droplet becomes concave, while the advancing side of the droplet remains convex, Fig. 6(b). Secondly, the weaker interfacial tension allows the droplets to be formed more frequently. The formation frequency can be measured accurately using the optical detection system.

Fig. 7 shows the typical signals of the droplets detected by the APD. The micro-droplets are well recognized as a pulse in the time signal. In the case of pure water, the pulse is well defined with two peaks representing the two edges of the micro-droplet. While measurement with the CCD camera can not differentiate the two edges of the water droplet, a clear difference in peak heights can be observed clearly in the optical signal, Fig. 7(a). Decreasing the interfacial tension between the aqueous liquid and the carrier liquid changes the shape of the droplet significantly. The detected time signal confirms the deformation observed previously with the CCD camera. At higher flow rates, the kinetic energy dominates over the surface energy of the droplet. Fig. 7(b) depicts the signal of droplets of diluted detergent (volume ratio of 12.5×10^{-3}) at a flow rate of 50 μL/h. The instability in the droplet shape and even satellite droplets can be clearly observed in the time signal.

In order to investigate the impact of interfacial tension on the droplet shape, aqueous liquids was prepared with different volume ratios between detergent and DI water. The higher the ratio, the lower is the interfacial tension between the aqueous liquid and the carrier liquid. Fig. 8 shows the effect of detergent/water ratio on the interfacial tension and subsequently on the radius of curvature at the two ends of the droplet. The droplets are formed at the same flow rate of 10 μL/h. From images recorded by the CCD camera we can clearly observe, that both sides of a pure-water droplet are convex, Fig. 6(a). This fact is represented well in the detected time signal shown in Fig. 8(a). The slight difference at the two edges is caused by the dynamic effect of a moving droplet.

With a high interfacial tension in the case of pure water, the difference between the advancing and receding sides of the droplet is minimum. As shown in Fig. 8(b–d), this difference increases with decreasing interfacial tension. The droplet transforms from an almost symmetric shape into a "bullet-like" shape as shown in Fig. 6(b). Fig. 9 depicts the corresponding time-differential signal ds/dt of the original signal $s(t)$ shown in Fig. 8. In practice, the time-differential signal can be obtained using a differentiator circuit. The positive and negative peaks of the time-differential signal represent the maximum slopes at the receding edge and advancing edge, respectively. The time-differential signal can be used for evaluating the shape of each

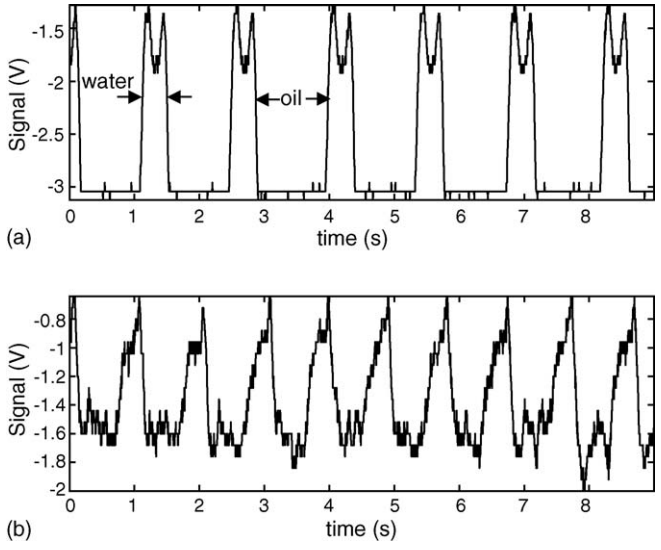

Fig. 7. Time signals of micro-droplets received by the APD (flow rate of the aqueous liquid is 50 μL/h): (a) pure DI water, (b) detergent diluted in DI water with a volume ratio of 12.5×10^{-3}.

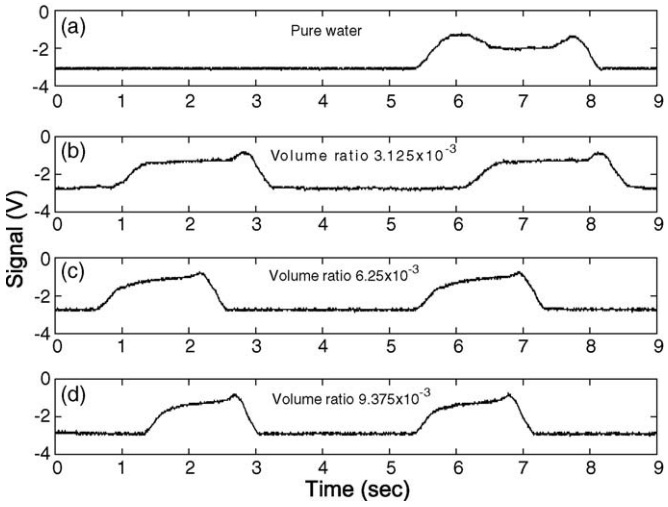

Fig. 8. Time signal $s(t)$ of sample droplet with different surfactant concentration (flow rate of the aqueous liquid: 10 μL/h).

droplet edge. The gap between the positive peak and the negative peak of the signals shown in Fig. 9 is a measure of the size of the droplet.

4.2. Droplet size

As mentioned above, the droplet size can be measured by the gap between the positive peak and the negative peak in the time-differential signal. From the analytical model, the size of the droplets is determined mainly by the interfacial tension and the flowrate. Eq. (4) shows that the droplet diameter is inversely proportional to the mean velocity of the carrier liquid ($D_d \propto 1/U_c$), and proportional to the square root of the interfacial tension ($D_d \propto \sqrt{\sigma}$). The interfacial tension is supposed to be inversely proportional to the detergent concentration. Thus droplet size will decrease with increasing detergent's volume ratio.

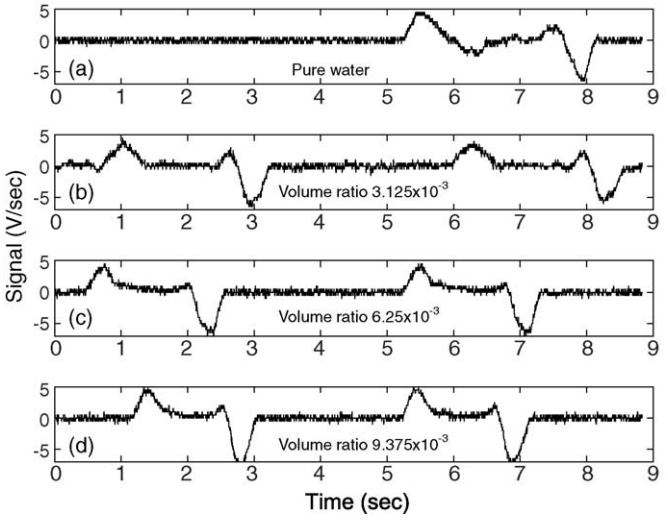

Fig. 9. The time-differential signal ds/dt of the signals shown in Fig. 8 (flow rate of the aqueous liquid: 10 μL/h).

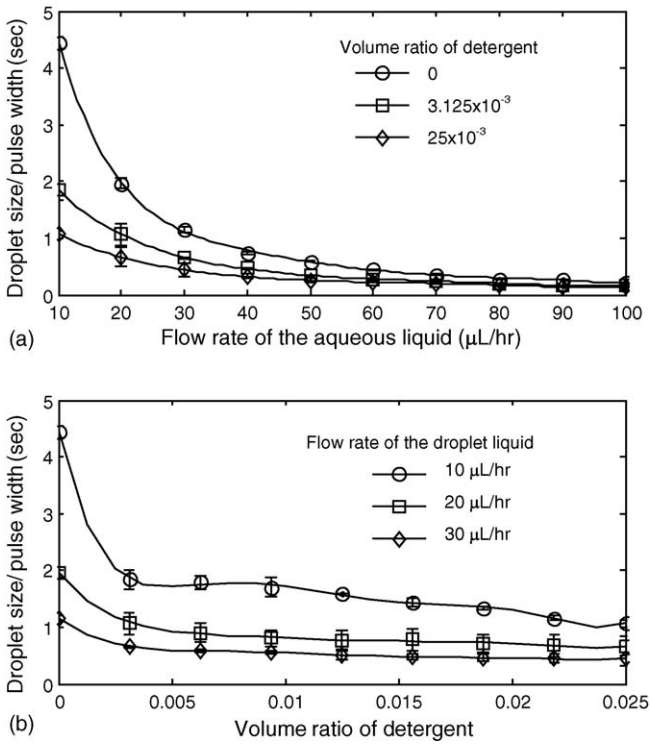

Fig. 10. Detected droplet size as function of (a) flow rate of the aqueous liquid and (b) volume ratio of detergent to pure water (solid lines are sixth order polynomial fitting functions).

The results shown in Fig. 10 confirm the behavior of droplet size expected from the theory. Droplet size or the pulse width of the time signal decrease with increasing flow rate of the aqueous liquid, Fig. 10(a). Since the flow rate ratio between the aqueous liquid and the carrier liquid was kept constant at 1:2, the droplet size is inversely proportional to the flow rate or the mean velocity of the carrier flow. Increasing the volume ratio between detergent and water decreases its interfacial tension to the carrier liquid and allows the droplets to form at smaller diameters, Fig. 10(b).

4.3. Formation frequency

The droplet formation process results from the balance between the drag force and the interfacial tension force. If the drag force on the droplet is higher then the interfacial tension, the droplet is released. Thus on the one hand, a higher drag force or a higher flow rate of the carrier flow leads to a higher formation frequency. On the other hand, a higher surfactant concentration or a lower interfacial tension also lead to a higher formation frequency. Eq. (4) predicts that the droplet formation frequency is proportional to the forth power of the mean velocity of the carrier liquid ($f \propto U_c^4$), and inversely proportional to the 3/2-th power of the interfacial tension ($f \propto 1/\sigma^{3/2}$). Fig. 11(a) shows the relation between the measured formation frequency and the flow rate of the aqueous liquid. The solid lines are fourth order polynomial fitting functions. Higher detergent's volume ratio leads to lower interfacial tension, and consequently higher formation frequency, Fig. 11(b). We can also observe that the error bars are wider at higher flow rates and higher detergent's volume ratios.

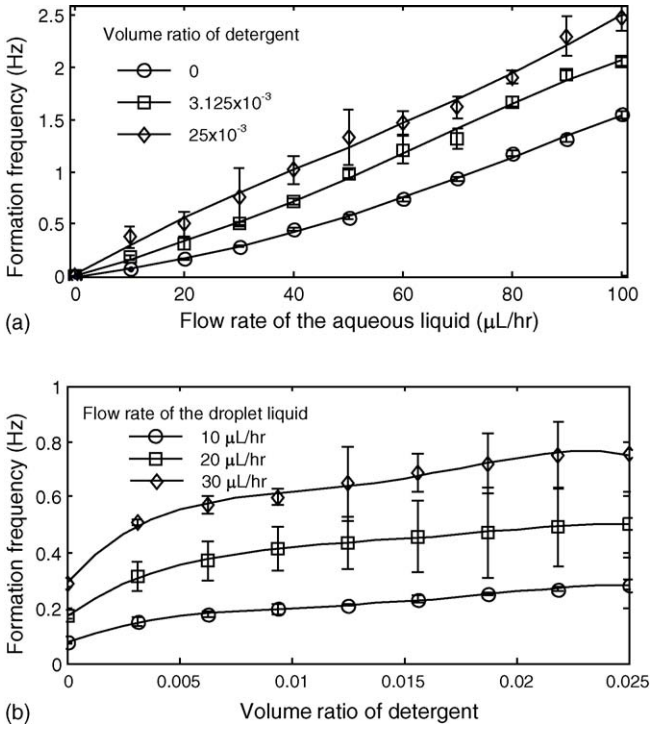

Fig. 11. Droplet formation frequency as function of (a) flow rate of the aqueous liquid and (b) volume ratio between detergent and pure water (solid lines are fourth order polynomial fitting functions).

In these two cases, the kinetic energy dominates over the surface energy of the droplets. Thus, the noise in the time signal is caused by the instability of the droplet shape and the formation of satellite droplets as shown earlier in Fig. 7.

5. Conclusions

This paper reports a microfluidic device for droplet formation and detection. The device has a microchannel network to form the droplets. The droplets are detected optically by two optical fibers. A droplet passing by the detection point diffracts a part of the incoming laser light and can be detected by the fiber placed on the other side of the channel. The device has a potential for feedback control in a droplet-based microfluidic device. Currently, droplet size, shape, and formation frequency can be measured accurately. The device can detect droplets at very high formation frequencies, where observation with a CCD camera and a microscope is not possible. The system can possibly detect the extent of mixing processes as well as chemical reactions inside droplets, which may be useful for adsorption analysis of biochemical samples.

Acknowledgment

This work was supported by the academic research fund of the Ministry of Education Singapore, contract number RG11/02.

References

[1] K. Handique, M.A. Burns, Mathematical modeling of drop mixing in a slit-type microchannel, J. Micromech. Microeng. 11 (2001) 548–552.
[2] P. Paik, V.K. Pamula, R.B. Fair, Rapid droplet mixers for digital microfluidic systems, Lab Chip 3 (2003) 253–259.
[3] T. Taniguchi, T. Torii, T. Higuchi, Chemical reactions in microdroplets by electrostatic manipulation of droplets in liquid media, Lab Chip 2 (2002) 19–23.
[4] H. Song, M.R. Bringer, J.D. Tice, C.J. Gerdts, R.F. Ismagilov, Experimental test of scaling of mixing by chaotic advection in droplets moving through microfluidic channels, Appl. Phys. Lett. 83 (2003) 4664–4666.
[5] T. Nisisako, T. Torii, T. Higuchi, Droplet formation in a microchannel network, Lab Chip 2 (2002) 24–26.
[6] S. Okushima, T. Nisisako, T. Torii, T. Higuchi, Controlled production of monodisperse double emulsion by two-step droplet breakup in microfluidic devices, Langmuir 20 (2004) 9905–9908.
[7] A.S. Utada, E. Lorenceau, D.R. Link, P.D. Kaplan, H.A. Stone, D.A. Weitz, Monodisperse double emulsions generated from a microcapillary device, Science 308 (2005) 537–541.

Biographies

Nam-Trung Nguyen was born in Hanoi, Vietnam, in 1970. He received his Dip-Ing, Dr Ing and Dr Ing Habil degrees from Chemnitz University of Technology, Germany, in 1993, 1997 and 2004, respectively. In 1998 he worked as a postdoctoral research engineer in the Berkeley Sensor and Actuator Center (UC Berkeley, USA). Currently he is an associate professor with the School of Mechanical and Aerospace Engineering of the Nanyang Technological University in Singapore. His research is focused on microfluidics and instrumentation for biomedical applications. He published a number of research papers on microfluidics. The second edition of his book "*Fundamentals and Applications of Microfluidics*" co-authored with S. Wereley will be published in summer 2006.

Sumantri Lassemono was born in Indonesia. He is currently competing his undergraduate study at the School of Mechanical and Aerospace Engineering of the Nanyang Technological University in Singapore.

Franck Alexis Chollet received his electronics engineering degree from the ENSERB, Bordeaux, France in 1991, and his doctorate degree in Sciences Pour lIngénieur from the Université de Franche-Comte, Besançon, France, in 1995 for his work on integrated optics devices for the CNET (France Telecom). He was then with LIMMS, a French Japanese laboratory, for two years at the IIS, University of Tokyo, Japan, as a JSPS post-doctoral fellow, where he developed optical MEMS. After a short stay at LPMO, Besançon, France, working on micro-cooler and LIGA process, he became a research associate at the IMRE, Singapore, where he worked on MEMS optical sensors and switches. Since September 1999 he is associate professor in the school of Mechanical and Aerospace Engineering at Nanyang Technological University, Singapore, and is the Vice-Director of the MicroMachines Centre where he pursues his work on optical MEMS and micro/nano fabrication technology.